International Journal of Ocean System Engineering 1(1) (2011) 16-27
DOI 10.5574/IJOSE.2011.1.1.016

Controller design for an autonomous underwater vehicle using nonlinear observers†

Shahriar Negahdaripour[1], Sohyung Cho[2] and Joon-Young Kim[3*]

[1]*Department of Electrical and Computer Engineering, University of Miami, Coral Gables, FL 33124, USA*
[2]*Department of Industrial and Manufacturing Engineering, Southern Illinois University, Edwardsville, IL 62026-1805, USA*
[3]*Department of Ocean System Engineering, Jeju National University, Jeju 690-756, Korea*

(Manuscript Received December 1, 2010; Revised January 2, 2011; Accepted February 7, 2011)

Abstract

The depth and heading control of an autonomous underwater vehicle (AUV) are considered to follow the predetermined depth and heading angle. The proposed control algorithm was based on a sliding mode control, using estimated hydrodynamic coefficients. The hydrodynamic coefficients were estimated employing conventional nonlinear observer techniques, such as sliding mode observer and extended Kalman filter. Using the estimated coefficients, a sliding mode controller was constructed for a combined diving and steering maneuver. The simulated results of the proposed control system were compared with those of a control system that employed true coefficients. This paper demonstrated the proposed control system, and discusses the mechanisms that make the system stable and accurately follow the desired depth and heading angle in the presence of parameter uncertainty.

Keywords: Autonomous underwater vehicle (AUV), Hydrodynamic coefficients, Extended Kalman filter, Sliding mode observer, Sliding mode control

1. Introduction

In recent years, intensive efforts have focused on the development of autonomous underwater vehicles (AUVs). In order to design an AUV, it is usually necessary to analyze its maneuverability and controllability based on a mathematical model. The mathematical model for most 6 DOF (degrees of freedom) contains hydrodynamic forces and moments expressed in terms of a set of hydrodynamic coefficients. Therefore, in order to correctly simulate the performance of an AUV, it is important to know the true values of these coefficients.

The hydrodynamic coefficients constitute the heart of the primary mathematical model used in simulation studies of the rigid-body motions of AUVs. These coeffici`ents are usually considered to be constant and independent of vehicle motion parameters. A number of mathematical models have been developed, particularly for AUVs, where the number and type of hydrodynamic coefficients differ, depending on the modeling of the forces and moments, e.g. the quadratic form, the cubic form and the combined quadratic-cubic form, of the damping forces and moments. The various hydrodynamic coefficients that are used in the dynamic equations of motion may be classified into 3 types, these being the added mass coefficients, due to the inertia of the surrounding fluid, and the linear/nonlinear damping coefficients, which result from fluid viscosity effects; of which, the linear damping coefficients have the largest affect on the maneuverability of an AUV [1]. Sen [1] examined the influence of various hydrodynamic coefficients on the predicted quality of maneuverability of submerged bodies, and found that the coefficients with

†This paper was presented at the OCEANS 2001 conference, Hawaii, USA, November 2001.

*Corresponding author. Tel.: +82-64-754-3485, Fax.: +82-64-751-3480.
E-mail address: jkim@jejunu.ac.kr.

significant effects on the trajectories were the linear damping coefficients.

These coefficients are normally obtained experimentally test, numerical analysis or empirical formulae. Although the planar motion mechanism (PMM) test is the most popular among experimental test, the measured values are not completely reliable due to experimental difficulties and errors.

Another approach is the observer method, which estimates the hydrodynamic coefficients with the help of a model-based estimation algorithm. A representative observer method is the Kalman filter, which has been widely used in the estimation of hydrodynamic coefficients and state variables. Hwang [2], Kim [3], and Yoon [4] estimated the maneuvering coefficients of a ship, and identified the dynamic system of a maneuvering ship, using an extended Kalman filtering technique.

These estimated coefficients are not only used in the mathematical model to analyze an AUV's maneuvering performance, but also in a controller model to design an AUV's autopilot. Fossen and Blanke [5] designed a propeller shaft speed controller by using feedback from the axial water velocity in the propeller disc. Farrell and Clauberg [6] reported the successful control of a Sea Squirt vehicle, which used an extended Kalman filter as a parameter estimator, with pole placement, to design the controller. Yuh [7] described a functional form of the vehicle dynamic equations of motion, the nature of the loadings, and the use of adaptive control via online parameter identification.

Recently, advanced control techniques have been developed for AUVs, with the aim of improving the capability to track the desired position and attitude trajectories. In particularly, the sliding mode control has been successfully applied to AUV due to its good robustness for modeling uncertainty, variation under different operating conditions, and disturbance. Yoerger and Slotine [8] proposed a series of SISO continuous-time controllers by using the sliding mode technique on an underwater vehicle, and demonstrated the robustness of their control system via a computer simulation in the presence of parameter uncertainties. Cristi et al. [9] proposed an adaptive sliding mode controller for AUVs, based on the dominant linear model and the bounds of the nonlinear dynamic perturbations. Healey and Lienard [10] and Sur and Seo [11] described a 6 DOF model for the maneuvering of an underwater vehicle, and designed a sliding mode autopilot for the combined steering, diving, and speed control functions. Lea et al. [12] compared the performance of a root locus, fuzzy logic, and sliding mode control, which they tested using an experimental vehicle. Lee et al. [13] designed a quasi-sliding mode controller for an AUV in the presence of parameter uncertainties, with a long sampling interval.

In this paper, the depth and heading control of an AUV are presented in order to maintain the desired depth and heading angle in a towing tank. The proposed control algorithm represents a sliding mode control, using estimated hydrodynamic coefficients. The hydrodynamic coefficients were estimated, based on the nonlinear observer such as sliding mode observer (SMO) and extended Kalman filter (EKF). Because the system to be controlled is highly nonlinear, a sliding mode control is constructed to compensate for the effects of modeling nonlinearity, parameter uncertainty, and disturbance.

This paper is organized as follows: Section 2 describes the nonlinear observers for estimating the hydrodynamic coefficients. Section 3 presents a sliding mode control for the depth and heading control. Section 4 shows the simulated results. Finally, section 5 presents the conclusions of the MUUTV.

2. Estimation of the hydrodynamic coefficients

The coefficients with the most significant effects on the dynamic performance of an AUV were found to be the linear damping coefficients. In particular, twelve of the linear damping coefficients were considered as highly sensitive parameters, which have previously be represented in Sen [1] as M_q, M_{ds}, N_r, N_{dr}, N_v, Z_{ds}, Z_q, Y_{dr}, Y_r, Y_v, K_p and K_r.

In this paper, in order to estimate the sensitive coefficients, an estimated system based on a nonlinear observer was constructed, as illustrated in Fig. 1. The nonlinear observer block was composed of SMO and EKF, which are designed based on the AUV's 6 DOF equations of motion. Based on the measured signal of the AUV's motion, two nonlinear observers were developed for estimating the sensitive coefficients. The AUV block represents the real plant and includes a 6 DOF model of an NPS AUV II [10]. The value of the sensitive coefficients from this block was used as the true value and compared with those estimated.

In nonlinear observers, 6 DOF AUV equations of motion, and the augmented states for the linear damping coefficients, are included. Thus, the observer model describes the surge, sway, heave, and roll, pitch and yaw motions. The coordinate system is shown in Fig. 2. The 6 DOF equations of motion for the observer design were as follows [14]:

$$
\begin{aligned}
&m[\dot{u}-vr+wq-x_G(q^2+r^2)+y_G(pq-\dot{r})+z_G(pr+\dot{q})]=X\\
&m[\dot{v}+ur-wp+x_G(pq+\dot{r})-y_G(p^2+r^2)+z_G(qr-\dot{p})]=Y\\
&m[\dot{v}+ur-wp+x_G(pq+\dot{r})-y_G(p^2+r^2)+z_G(qr-\dot{p})]=Y\\
&I_x\dot{p}+(I_z-I_y)qr+I_{xy}(pr-\dot{q})-I_{yz}(q^2-r^2)\\
&-I_{xz}(pq+\dot{r})+m[y_G(\dot{w}-uq+vp)-z_G(\dot{v}+ur-wp)]=K\\
&I_y\dot{q}+(I_x-I_z)pr-I_{xy}(qr+\dot{p})+I_{yz}(pq-\dot{r})\\
&+I_{xz}(p^2-r^2)-m[x_G(\dot{w}-uq+vp)-z_G(\dot{u}-vr+wq)]=M\\
&I_z\dot{r}+(I_y-I_x)pq-I_{xy}(p^2-q^2)-I_{yz}(pr+\dot{q})\\
&+I_{xz}(qr-\dot{p})+m[x_G(\dot{v}+ur-wp)-y_G(\dot{u}-vr+wq)]=N
\end{aligned}
\tag{1}
$$

where u, v and w are the velocities of the surge, sway and heave motion, and p, q and r the angular velocities of the roll, pitch, and yaw motion, respectively. X, Y, Z, K, M and N represent the resultant forces and moments with respect to the x, y and z axes, respectively; their detailed expressions and nomenclatures have previously been described in [14]. In order to estimate the linear damping coefficients, they have to be modeled as extra state variables. Consequently, Eq. (1), the 6 DOF equations of motion, is transformed into an augmented state-space form as follows:

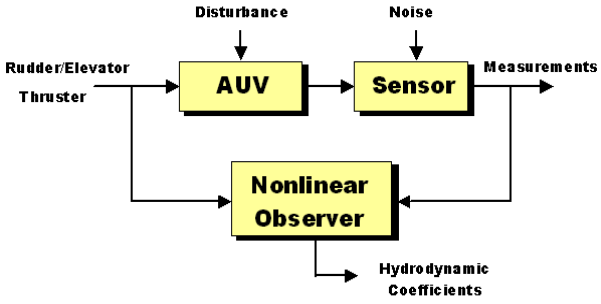

Fig. 1. Configuration of the estimate system

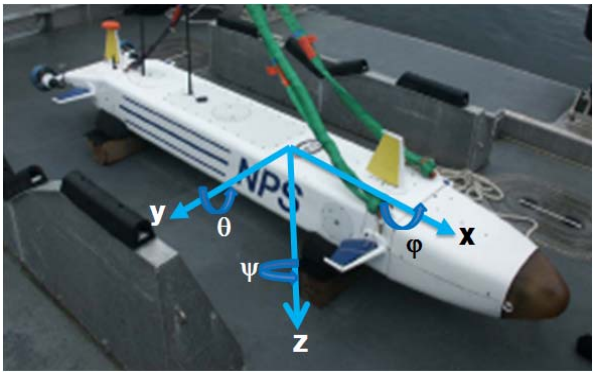

Fig. 2. Coordinate system

$$
[M]\begin{bmatrix}\dot{u}\\ \dot{v}\\ \dot{w}\\ \dot{p}\\ \dot{q}\\ \dot{r}\\ \dot{\phi}\\ \dot{\theta}\\ \dot{\psi}\\ \dot{\xi}\end{bmatrix}=\begin{bmatrix}X_e+X_m\\ Y_e+Y_m\\ Z_e+Z_m\\ K_e+K_m\\ M_e+M_m\\ N_e+N_m\\ p+q\sin\phi\tan\theta+r\cos\phi\tan\theta\\ q\cos\phi-r\sin\phi\\ (q\sin\phi+r\cos\phi)\sec\theta\\ 0\end{bmatrix} \tag{2}
$$

where $M\in R^{21\times21}$ is the inertia matrix, with a hydrodynamic added mass, and the extra state $\xi\in R^{21\times1}$, denotes the linear damping coefficients. The ϕ, θ and ψ are the angles of roll, pitch and yaw respectively. X_e, Y_e, Z_e, K_e, M_e and N_e represent the external forces and moments, except the added mass term. X_m, Y_m, Z_m, K_m, M_m, and N_m stand for the components of the inertial terms transposed from the left hand-side of Eq. (1). Especially, the added mass coefficients and the nonlinear damping coefficients in Eq. (2) were taken from the NPS AUV II [10] as known values. Therefore, nonlinear observers were designed based on Eq. (2).

2.1 Sliding mode observer (SMO)

The SMO, which was developed on the basis of the sliding surface concept, can set the gain value according to a uncertainty range of the plant model. The SMO is known to be robust under parameter uncertainty and disturbance. In addition, it can be easily applied to a nonlinear system [15]. In general, a nonlinear system may be represented by:

$$\dot{x} = f(x,t)$$
$$y = Cx \tag{3}$$

where $x \in R^n$ is the state vector, $y \in R^m$ the measurement vector, the true plant and $C \in R^{m \times n}$ the measurement matrix. The measurement is assumed to be a linear combination of the state, with the inputs contained in $f(x,t)$. If we define a sliding surface is defined as the error $\tilde{y}$,

$$s = \tilde{y} = \hat{y} - y = C(\hat{x} - x) \tag{4}$$

the sliding surface will then converge to zero when it satisfies the Lyapunov stability, as follows:

$$s\,\dot{s} = \tilde{y}\,\dot{\tilde{y}} < 0 \tag{5}$$

Eq. (5) is referred to as the sliding condition. If Eq. (5) is satisfied, the sliding $s = 0$ is guaranteed and the error $\tilde{y}$ tends toward zero. In order to satisfy the sliding condition, the SMO is given by:

$$\dot{\hat{x}} = f(\hat{x},t) - L\,\tanh(\tilde{y}/\Phi) \tag{6}$$

where L is the nonlinear gain matrix to be determined and $\tanh(\tilde{y}/\Phi)$ represents the switching term, which uses the 'tanh' function, instead of 'sign' function. Φ is the boundary layer thickness, which acts as a low-pass filter to remove chattering and noise. From Eq. (3) and Eq. (6), the error dynamics are given by:

$$\begin{aligned}\dot{\tilde{x}} &= \dot{\hat{x}} - \dot{x} \\ &= f(\hat{x},t) - f(x,t) - L\,\tanh(\tilde{y}/\Phi) \\ &= \Delta f(\tilde{x},t) - L\,\tanh(\tilde{y}/\Phi)\end{aligned} \tag{7}$$

where $f(\hat{x},t)$ is the modeled plant. The value of $\Delta f(\tilde{x},t)$ depends both on the modeling complexity and the magnitude of the error. Using the error dynamics, Eq. (7), the sliding condition is as follows:

$$\tilde{y}\,\dot{\tilde{y}} = \tilde{y}\,C\,\dot{\tilde{x}} = \tilde{y}\,C(\Delta f - L\tanh(\tilde{y}/\Phi)) < 0 \tag{8}$$

To satisfy Eq. (8), given bounds on Δf, the nonlinear gain, L, is chosen by:

$$L_i > \left|\Delta f_i(\tilde{x},t)\right| \quad , \quad (i = 1 \sim p) \tag{9}$$

Here L_i is the pth order nonlinear gain. In addition, during sliding, namely when the sliding surface goes to zero, the switching term can be written from Eq. (8):

$$\tanh(\tilde{y}/\Phi) \approx (CL)^{-1} C\Delta f \tag{10}$$

From Eq. (10), the error dynamics, Eq. (7), is developed by:

$$\dot{\tilde{x}} \approx \left[I - L(CL)^{-1}C\right]\Delta f \tag{11}$$

where I implies the identity matrix. Therefore, the system dynamics are reduced from the *n*th to the *n-p*th order during sliding. The above Eq. (11) has the form of $\dot{\tilde{x}} = a\tilde{x}$; therefore, the nonlinear gain matrix L is chosen, such that has a negative eigenvalue. In order to estimate the hydrodynamic coefficients, the SMO was designed using the observer model Eq. (2). The state variable yields $x = [u\ v\ w\ p\ q\ r\ \phi\ \theta\ \psi\ M_q\ M_{ds}\ N_r\ N_{dr}\ N_v\ Z_{ds}\ Z_q\ Y_{dr}\ Y_r\ Y_v\ K_p\ K_r]^T$. The output variables were chosen as $y = [u\ v\ w\ p\ q\ r\ \phi\ \theta\ \psi\ ]^T$.

2.2 Extended kalman filter (EKF)

The EKF can optimally estimate the state variables in nonlinear stochastic cases, which include plant perturbation and sensor noise. In particular, unknown inputs or parameters can be estimated by their conversion to extra state variables [16]. Assuming a system containing unknown parameters is given as follows:

$$\begin{aligned}x_{k+1} &= f(x_k, \xi_k, k) + w_k \\ y_k &= h(x_k, \xi_k, k) + v_k\end{aligned} \tag{12}$$

where $x \in R^n$ is the state vector, $y \in R^m$ the measurement vector, $\xi \in R^p$ the unknown parameter vector, w the plant disturbance, and v is the sensor noise. In order to estimate the unknown parameters, the state variable, x, is augmented by the unknown parameters. Therefore, Eq. (12) can be

expressed in an augmented state-space form as follows:

$$x_{k+1}^{*} = \begin{bmatrix} x_{k+1} \\ \xi_{k+1} \end{bmatrix} = \begin{bmatrix} f(x_k, \xi_k, k) \\ 0 \end{bmatrix} + \begin{bmatrix} w_k \\ \eta_k \end{bmatrix}$$
$$y_k = h(x_k^{*}, k) + v_k \tag{13}$$

where $w \in R^n$, $\eta \in R^p$ and $v \in R^m$ are zero-mean Gaussian white noise sequences and $x^{*} \in R^{n+p}$ is the augmented state vector. For this system, the discrete time EKF is summarized as

Time update:

$$\hat{x}_{k+1}^{*}(-) = f(\hat{x}_k^{*}(+), k) \tag{14}$$
$$P_{k+1}(-) = F_k^{*} P_k(+) F_k^{*T} + Q_k \tag{15}$$

Measurement update:

$$K_k = P_k(-) H_k^{*T} \left[H_k^{*} P_k(-) H_k^{*T} + R_k \right]^{-1} \tag{16}$$
$$\hat{x}_k^{*}(+) = \hat{x}_k^{*}(-) + K_k \left[y_k - h(\hat{x}_k^{*}(-), k) \right] \tag{17}$$
$$P_k(+) = \left[I - K_k H_k^{*} \right] P_k(-) \tag{18}$$

where $F_k^{*} = \left. \frac{\partial f(x^{*}, k)}{\partial x^{*}} \right|_{x^{*} = \hat{x}_k^{*}(+)}$, $H_k^{*} = \left. \frac{\partial h(x^{*}, k)}{\partial x^{*}} \right|_{x^{*} = \hat{x}_k^{*}(-)}$

P is the error covariance and Q the process noise covariance. The gain matrix, K, is determined from the Riccati equation, and the measurement noise covariance, R, is determined by satisfying the Lyapunov function of error [17]. P and Q are determined by scaling the fixed magnitude [18]. Time updates, Eq. (14) and Eq. (15) represent the extrapolation by the state transition matrix and measurement updates Eq. (16), Eq. (17) and Eq. (18) reflect the actual measurement process due to optimal gain .

To estimate the hydrodynamic coefficients, the EKF was designed using the observer model of Eq. (2). The 12 linear damping coefficients, which are represented by, are estimated using Eq. (14) - (18). The state and output variables were equal to those of the SMO.

2.3 Estimation results

In order to estimate the twelve sensitive coefficients associated with the horizontal and vertical motions, a simulation was conducted for the combined diving and steering motion of the AUV. The sensitive coefficients from the AUV block in Fig. 1 were used as true values and compared with those estimated. The performances of the SMO and the EKF estimation were compared when the AUV underwent combined diving and steering. The motion scenario was as follows: the AUV has the initial speed of 1.8m/sec, with a rudder/ elevator angle applied to 20˚ from the start. The rudder and elevator work within -23˚ to 23˚. Fig. 3 shows the rudder/elevator angles, the velocities and the 3-D trajectory of the motion scenario.

Table 1. Steady-state error (%)

	SMO	EKF
M_q	1.10	0.12
M_{ds}	1.46	0.26
N_r	24.67	0.33
N_{dr}	17.78	0.58
N_v	30.35	0.13
Z_{ds}	3.07	0.05
Z_q	2.48	0.09
Y_{dr}	49.34	14.53
Y_r	102.57	9.61
Y_v	44.22	23.29
K_p	0.09	0.14
K_r	5.28	0.01

Figs. 4 - 8 compare the results estimation via the SMO and EKF for the twelve sensitive coefficients. The steady-state error has been compared in Table 1. In the figures, a thick solid line represents the true value adopted from [10], and the dashed/solid line those of the SMO/EKF results. In general, the EKF exhibited a good estimation performance, but Y_{dr}, Y_r and Y_v, which are associated with sway motion, contained steady-state errors. The SMO is well known to be a robust observer under parameter uncertainty and disturbance, but has large steady-state errors and fluctuations during the transient period. Based on a series of simulations, the EKF was concluded to estimate the sensitive coefficients

with sufficient accuracies. Although the nonlinear observers were used off-line in order to analyze system identification, they can be implemented on-line to estimate the state variables and control of an AUV.

In this paper, nonlinear observers for estimating the hydrodynamic coefficients exhibited a good performance as the input data for the observer were taken from the simulated results of the NPS AUV II. However, the estimated coefficients were expected to contain many when the input data are taken from sea trial results. The sea trial data can be contaminated with sensor noise and contain complex terms due to coupled motion of an AUV.

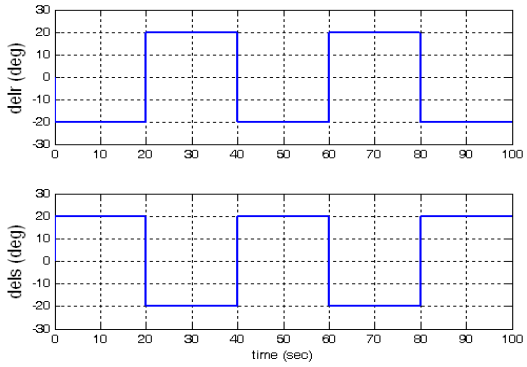

(a) steering and elevator angles

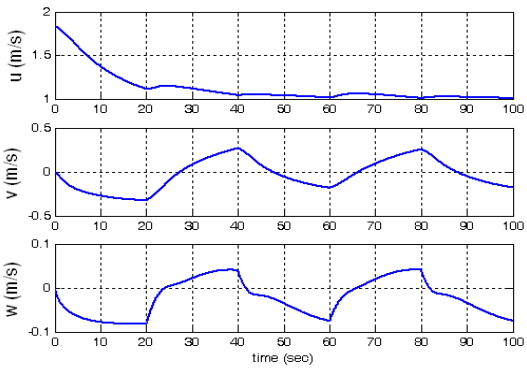

(b) surge, sway, and heave velocities

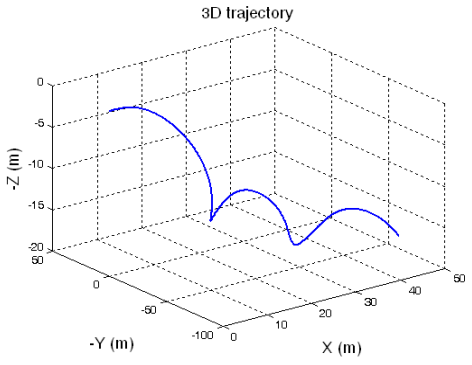

(c) 3-D trajectory

Fig. 3. Inputs and outputs of motion scenario

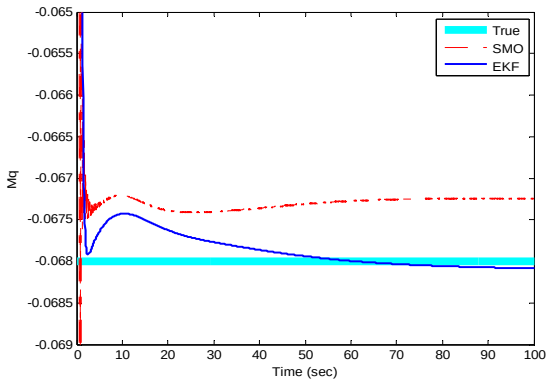

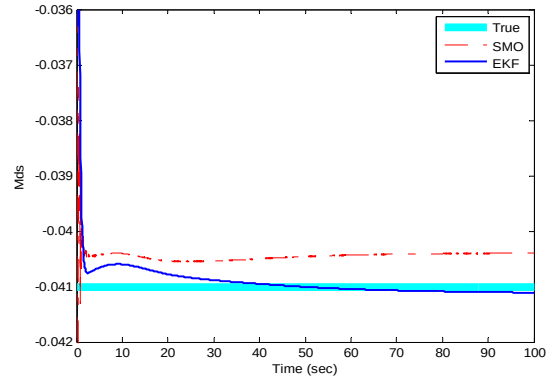

Fig. 4. Pitch coefficients M_q and M_{ds}

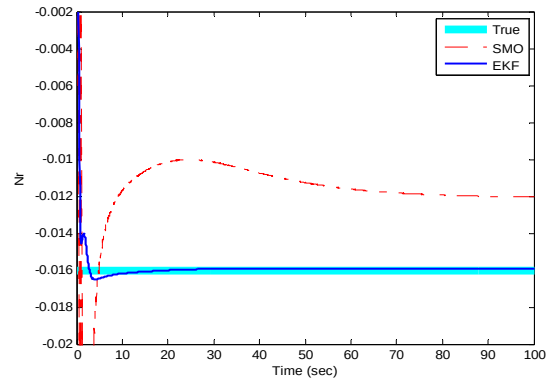

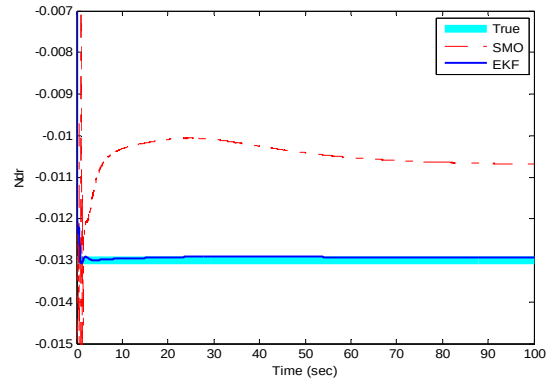

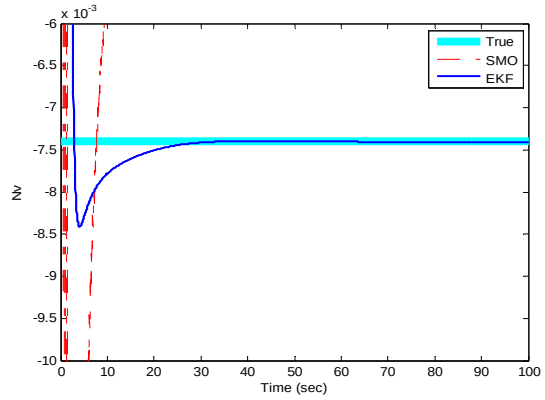

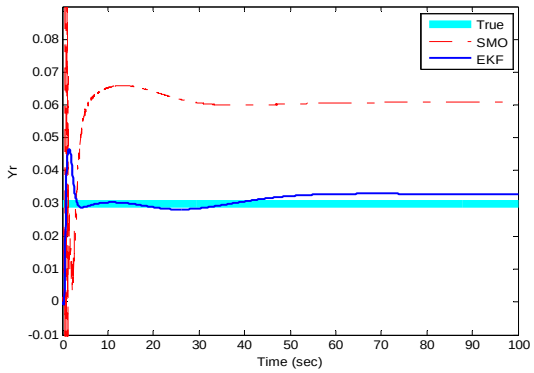

Fig. 5. Yaw coefficients N_r, N_{dr} and N_v

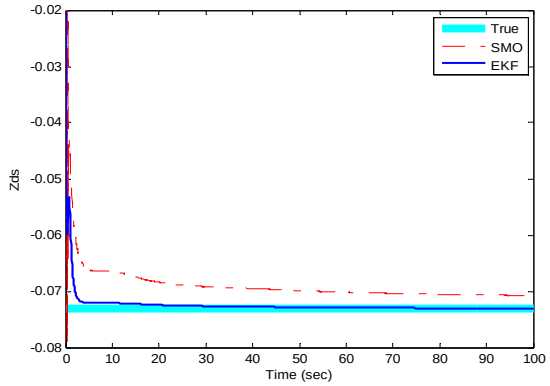

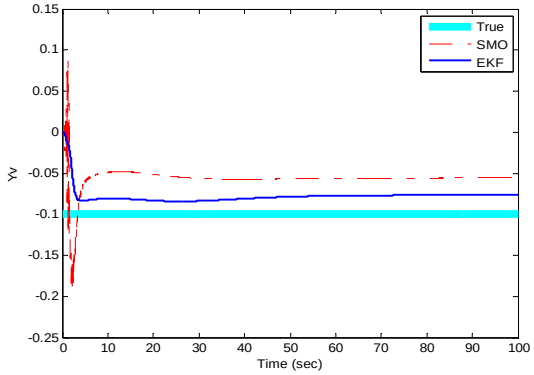

Fig. 7. Sway coefficients Y_{dr}, Y_r and Y_v

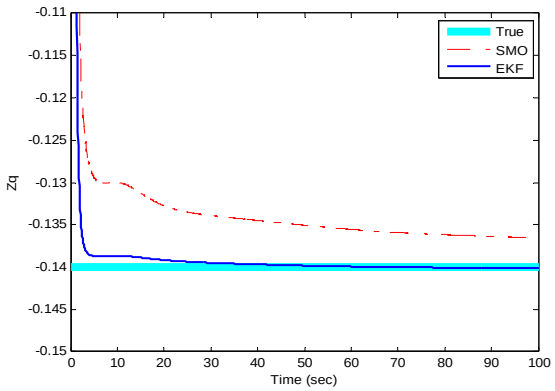

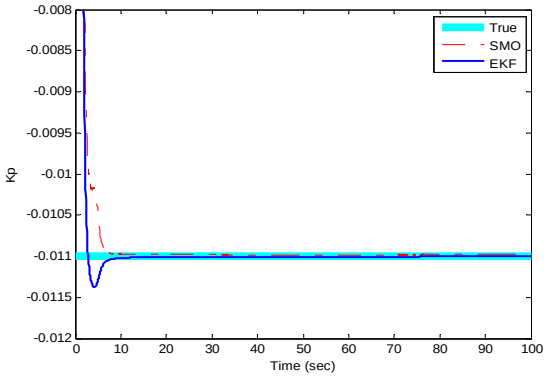

Fig. 6. Heave coefficients Z_{ds} and Z_q

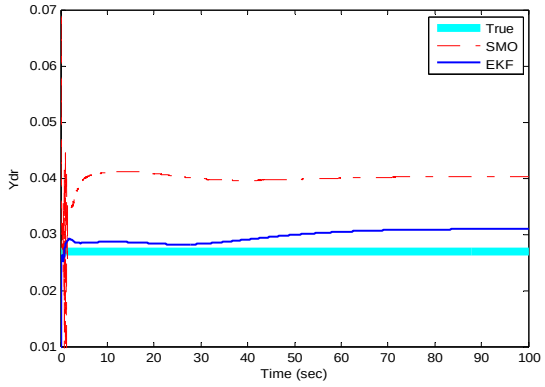

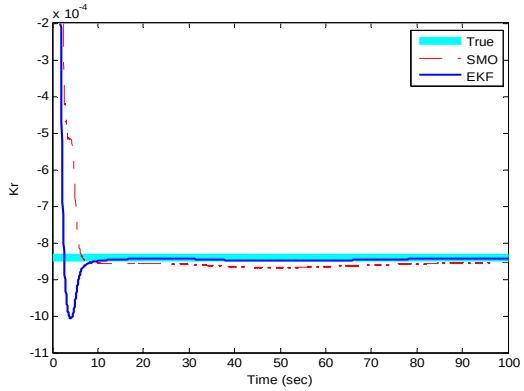

Fig. 8. Sway coefficients K_p and K_r

3. Controller design

Although an AUV system is difficult to control, due to high nonlinearity and motion coupling, sliding mode control has been successfully applied to underwater vehicles. In this paper, a sliding mode control was adopted for an AUV with uncertainty in the system parameters. Particularly, when designing a sliding mode controller, the estimated hydrodynamic coefficients in section 2 were applied to the controller model.

The sliding mode control is well to provide an effective and robust way of controlling uncertainty in plants by means of a switching control law, which drives the plant's state trajectory onto the sliding surface in the state space. With only a single control element active, each subsystem may be treated separately as a single input, multi-state system, with its own single sliding surface definition. Any system can be described as a single input, multi-state equation [10].

$$\dot{x}(t) = Ax(t) + bu(t) + \delta f(t)$$
$$x(t) \in R^{n\times 1},\ A \in R^{n\times n},\ b \in R^{n\times 1} \tag{19}$$

where $\delta f(t)$ is a nonlinear function, which describes the disturbances and unmodelled coupling effects. The sliding surface is defined as:

$$\sigma = s^T \tilde{x} \tag{20}$$

where s^T represents the sliding surface coefficient and $\tilde{x}$ the state error, *i.e.* $\tilde{x} = x - x_d$. It is important that the sliding surface is defined such that as the sliding surface tends toward zero, and the state error also tends toward zero. The sliding surface reaches zero in a finite amount of time under the condition:

$$\dot{\sigma} = -\eta \,\mathrm{sgn}(\sigma) \tag{21}$$

where η represents the nonlinear switching gain. From Eq. (19) and Eq. (21), the following is obtained:

$$s^T(Ax + bu + \delta f - \dot{x}_d) = -\eta \,\mathrm{sgn}(\sigma) \tag{22}$$

and the control input determined as follows:

$$u = -(s^T b)^{-1} s^T Ax + (s^T b)^{-1}[-s^T \delta f + s^T \dot{x}_d - \eta \,\mathrm{sgn}(\sigma)] \tag{23}$$

If the pair, (A, b), is controllable and $(s^T \mathrm{b})$ is nonzero, then it may be shown that the sliding surface coefficients are the elements of the left Eigenvector of the closed-loop dynamics matrix, $(A - \mathrm{b}k^T)$, corresponding to a pole at the origin:

$$s^T[A - bk^T] = 0 \tag{24}$$

where the linear gain vector, k^T, is defined as $(s^T b)^{-1} s^T A$, which can be evaluated via a the standard method, such as pole placement. It should be mentioned that one of the Eigenvalues of $(A - bk^T)$ must be specified as being zero. The resulting sliding control law, using a '*tanh*' function, is given as:

$$u = -k^T x - (s^T b)^{-1} s^T \delta f + (s^T b)^{-1} s^T \dot{x} - \eta (s^T b)^{-1} \tanh(\sigma/\Phi) \tag{25}$$

where Φ is the boundary layer thickness, which it acts as a low-pass filter to remove chattering and noise. The choices of the nonlinear switching gain, η, and the boundary layer thickness, Φ, are selected to eliminate control chattering.

3.1 Depth control

In order to design a controller in the vertical plane, the linearized diving system dynamics were developed as follows:

$$\begin{aligned}(I_y - \frac{\rho}{2}L^5 M_{\dot{q}})\dot{q} &= (\frac{\rho}{2}L^4 u\hat{M}_q)q - (z_G - z_B)W\theta \\ &\quad + (\frac{\rho}{2}L^3 u^2 \hat{M}_{\delta s})\delta_s \\ \dot{\theta} &= q \\ \dot{Z} &= -u\theta\end{aligned} \tag{26}$$

In Eq. (26), the values of $\hat{M}_q$ and $\hat{M}_{\delta s}$ were taken as those estimated (EKF) in section 2. The dynamic model for the depth control yields the state equation as:

$$\begin{bmatrix}\dot{q}\\ \dot{\theta}\\ \dot{Z}\end{bmatrix}=\begin{bmatrix}-1.002 & -0.066 & 0\\ 1 & 0 & 0\\ 0 & -1.832 & 0\end{bmatrix}\begin{bmatrix}q\\ \theta\\ Z\end{bmatrix}+\begin{bmatrix}-0.209\\ 0\\ 0\end{bmatrix}\delta_s \tag{27}$$

The sliding surface is defined as:

$$\sigma_s = 28.18\tilde{q} + 14.37\tilde{\theta} - \tilde{Z} \tag{28}$$

where $\tilde{q}$, $\tilde{\theta}$, and $\tilde{Z}$ represent the errors associated with the pitch rate, pitch angle, and depth, respectively. When the poles are placed at [0 -0.25 -0.26]. The depth control law is finally determined as:

$$\delta_s = 2.3531q + 0.0062\theta - 0.1698\dot{Z}_d + 2.3\tanh(\sigma_s/4) \tag{29}$$

To implement the above depth control law, an AUV has to be equipped with the pitch rate, pitch angle and depth sensors.

3.2 Heading control

The linearized steering system dynamics are given as follows:

$$\begin{aligned}(m-\frac{\rho}{2}L^3Y_{\dot{v}})\dot{v}-(\frac{\rho}{2}L^4Y_{\dot{r}})\dot{r} &= (\frac{\rho}{2}L^2u\hat{Y}_v)v+(\frac{\rho}{2}L^3u\hat{Y}_r-mu)r\\ &\quad+(\frac{\rho}{2}L^2u^2\hat{Y}_{\delta r})\delta_r\\ -(\frac{\rho}{2}L^4N_{\dot{v}})\dot{v}+(I_z-\frac{\rho}{2}L^5N_{\dot{r}})\dot{r} &= (\frac{\rho}{2}L^3u\hat{N}_v)v+(\frac{\rho}{2}L^4u\hat{N}_r)r\\ &\quad+(\frac{\rho}{2}L^3u^2\hat{N}_{\delta r})\delta_r\\ \dot{\psi} &= r\end{aligned} \tag{30}$$

In Eq. (30), the values of $\hat{Y}_v$, $\hat{Y}_r$, $\hat{Y}_{\delta r}$, $\hat{N}_v$, $\hat{N}_r$ and $\hat{N}_{\delta r}$ were taken as those estimated (EKF). The dynamic model for heading control yields the state equation:

$$\begin{bmatrix}\dot{v}\\ \dot{r}\\ \dot{\psi}\end{bmatrix}=\begin{bmatrix}-0.209 & -0.605 & 0\\ -0.054 & -0.569 & 0\\ 0 & 1 & 0\end{bmatrix}\begin{bmatrix}v\\ r\\ \psi\end{bmatrix}+\begin{bmatrix}0.145\\ -0.152\\ 0\end{bmatrix}\delta_r \tag{31}$$

The values for placement of the poles of the steering system at [0 -0.41 -0.42] become:

$$\sigma_r = 0.15\tilde{v} + 1.65\tilde{r} + \tilde{\psi} \tag{32}$$

where $\tilde{v}$, $\tilde{r}$ and $\tilde{\psi}$ denote the errors of sway velocity, yaw rate and yaw angle, respectively. The heading control law is as follows:

$$\delta_r = 0.5260v + 0.1621r + 4.3465\psi_d + 1.5\tanh(\sigma_r/0.05) \tag{33}$$

In order to implement the above heading control law, it is necessary to measure the signals of lateral velocity, yaw rate and yaw angle.

4. Simulation results

Numerical simulations were performed to show the effectiveness of the proposed control system. The simulation program, which was developed using MATLAB 6.0, within the SIMULINK 4.0 environment, is shown in Fig. 8. The controller block was composed of a sliding mode controller and a PID controller for the depth and heading control. The input and output AUV, as the true plant, were taken from the NPS AUV II [10]. The depth and heading controls were simulated with the full nonlinear equation and the sliding mode controller developed in Eq. (29) and Eq. (33). The responses of the control law with the EKF values, which were almost the same as the true values were compared with those of the control law with the SMO values, which contained steady-state errors.

In addition, the performance of the sliding mode controller was compared with that of the PID controller. The traditional PID controller, with fixed gains, is well known as not being able to meet the requirements of underwater vehicle control.

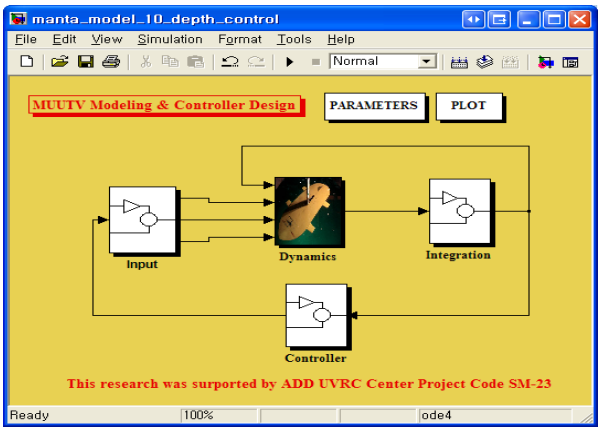

Fig. 9. SIMULINK model for control simulation

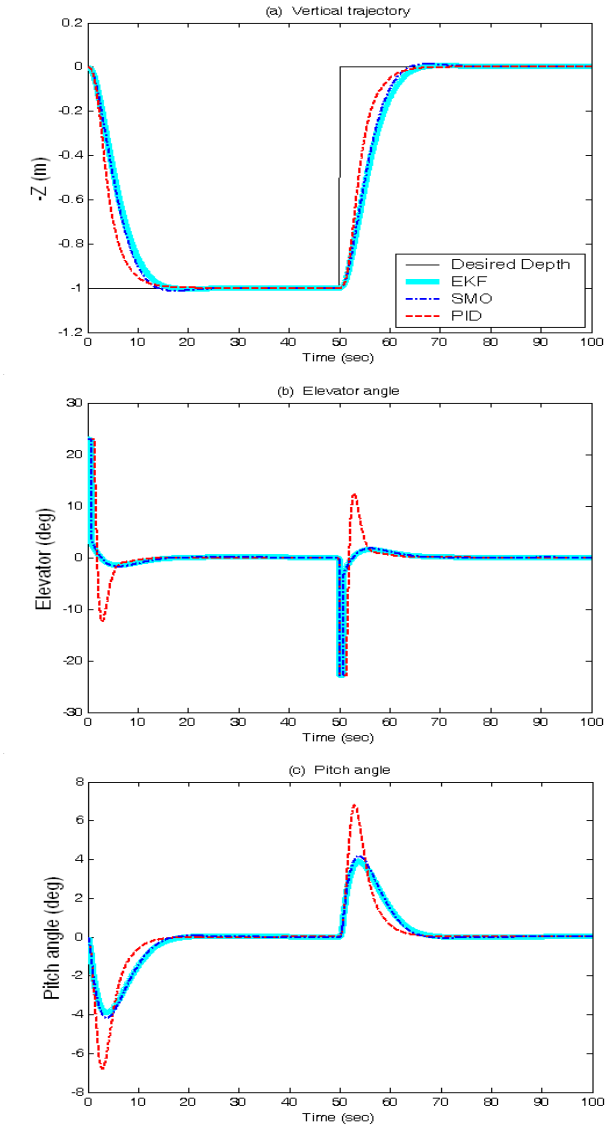

Fig. 10. Simulation results of depth control

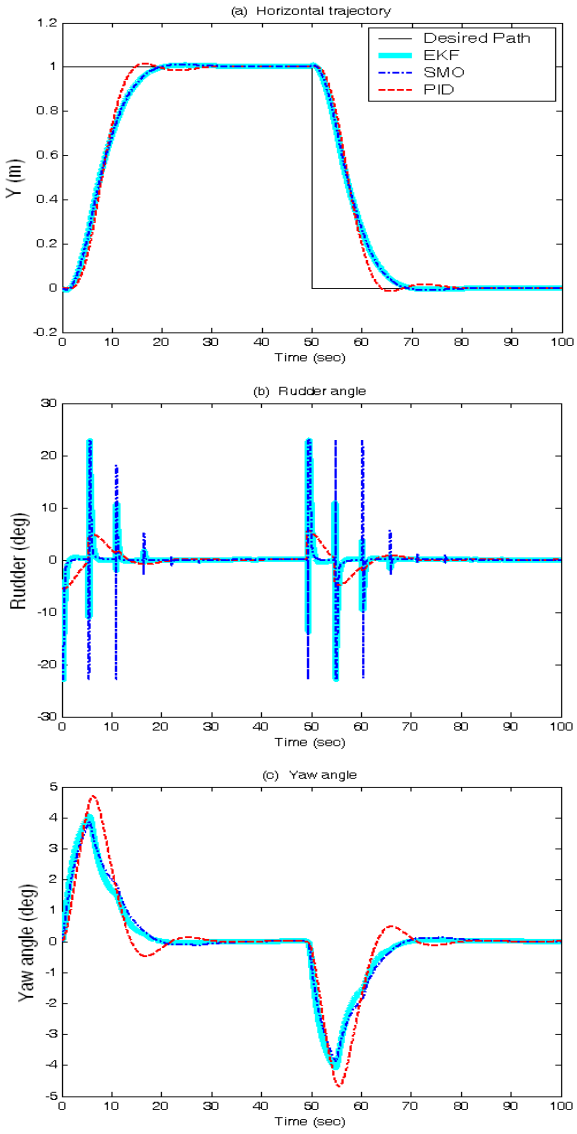

Fig. 11 Simulation results of heading control

However, the traditional PID controller and the modified PID controller with variable gains, were applied for an AUV in the field.

Fig. 9 shows the desired depth, tracking trajectory, and other controlled variables for the depth control simulation, which was carried out with the heading control to avoid the horizontal motion due to coupling. The desired depth was 1 m down from the initial depth during the first 50 secs, but then resumed the initial depth thereafter. From these figures, it was found that the performance of the controller with the SMO is similar to that of the controller with the EKF. The controller with the SMO exhibited particularly good tracking performance, deviations in the coefficients'.

This result means that the sliding mode control was robust, even under parameter uncertainty. In addition, the performance of the controller with a nonlinear observer was similar to that of the PID controller.

Fig. 10 shows the responses of the heading control, which was simulated with depth control to prevent the vertical motion due to coupling. To follow the desired path, the line of sight [10] was defined in terms of the desired yaw angle, and the proposed heading control will then follow the desired yaw angle. The desired path was chosen as 1 m towards the y-direction during the first 50 secs, and then returned to the initial position. In the figures, the controller with the SMO followed the desired path, which was similar to that of the control-

ler with the EKF, but required a slightly greater little more rudder angle, as shown in Fig. 10 (b). It is worth noting that the controller with the SMO follows the desired path, even when the estimated coefficients contained steady-state errors.

5. Conclusions

A sliding mode control, using estimated hydrodynamic coefficients, has been proposed in this paper to maintain the desired depth and heading angle. The hydrodynamic coefficients were estimated based on the nonlinear observers of the SMO and EKF. The EKF exhibited particularly good estimation performance, and estimated the coefficients with sufficient accuracy, although it contained steady-state errors. Using the estimated coefficients, a sliding mode controller was designed for the diving and steering maneuver. The control system with the SMO was compared to that with the EKF. The proposed control system is demonstrated to be stable and accurately follow the desired depth and path. This means that the sliding mode control showed robustness under parameter uncertainties. It is believed the proposed estimation method reduces the PMM test for measuring the hydrodynamic coefficients. In addition, the proposed control system makes the AUV stable and controllable in the presence of parameter uncertainties.

Acknowledgements

This research was supported by UVRC (Underwater Vehicle Research Center) and UTRC(Unmanned Technology Research Center) of ADD

References

[1] Sen Debabrata, *A Study on Sensitivity of Maneuverability Performance on the Hydrodynamic Coefficients for Submerged Bodies*, J. of Ship Research, 44 (3) (2000) 186-196.

[2] Wei-Yuan Hwang, *Application of System Identification to Ship Maneuvering*, Ph.D. Thesis, MIT, (1980).

[3] C.K. Kim, *Estimation of Manoeuvring Coefficients of a Submerged Body by Parameter Identification*, Ph.D. Thesis, Seoul National University, (1996).

[4] H.K. Yoon, *Estimation of Hydrodynamic Coefficients Using the Estimation-Before-Modeling Technique*, Ph.D. Thesis, Seoul National University, (2003).

[5] Thor I. Fossen, and Mogens Blanke, *Nonlinear Output Feedback Control of Underwater Vehicle Propellers Using Feedback from Estimated Axial Flow Velocity*, IEEE J. of Oceanic Eng., 25 (2) (2000) 241-255.

[6] Jay Farrell and Bernd Clauberg, *Issues in the Implementation of an Indirect Adaptive Control System*, IEEE J. of Oceanic Eng., 18 (3) (1993) 311-318.

[7] J. Yuh, *Modeling and Control of Underwater Vehicles*, IEEE Trans. on Syst,, Man, Cybern., 20 (1990) 1475-1483.

[8] Dana R. Yoerger, and Jean-Jacques E. Slotine, James B. Newman, Hagen Schempf, *Robust Trajectory Control of Underwater Vehicles*, IEEE J. of Oceanic Eng., OE-10 (4) (1985) 462-470.

[9] Roberto Crist, Fotis A. Papoulia, and Anthony J. Healey, *Adaptive Sliding Mode Control of Autonomous Underwater Vehicles in the Dive Plane*, IEEE J. of Oceanic Eng., 15 (3) (1990) 152-160.

[10] Anthony J. Healey and David Lienard, *Multivariable Sliding Mode Control for Autonomous Diving and Steering of Unmanned Underwater Vehicles*, IEEE J. of Oceanic Eng., 18 (3) (1993) 327-339.

[11] J. N. Sur, and Y. T. Seo, *Design and Experimental Evaluation of Sliding Mode Controller for Nonlinear Autonomous Underwater Vehicle*, J. of Ocean Engineering and Technology, 6 (1) (1992) 11-18.

[12] R.K. Lea, R. Allen, and S.L. Merry, *A Comparative Study of Control Techniques for an Underwater Flight Vehicle*, International J. of System Science, 30 (9) (1999) 947-964.

[13] Pan-Mook Lee, Bong-Hwan Jeon, and Seok-Won Hong, *Quasi-Sliding Mode Control of an Autonomous Underwater Vehicle with Long Sampling Interval*, J. of Ocean Engineering and Technology Eng., 12 (2) (1998) 130-138.

[14] Thor I. Fossen, *Guidance and Control of Ocean Vehicles*, John Wiley & Sons (1994).

[15] J. J. E. Slotine, J. K. Hedrick, and E. A. Misawa, *On Sliding Observers for Nonlinear Sys-*

tems, ASME J. of Dynamics, Measurement, and Control, 109 (1987) 245-252.

[16]Laura R. Ray, *Stochastic Decision and Control Parameters for IVHS*, ASME IMECE Advanced Automotive Technologies, (1995) 114-118.

[17]M. Boutayeb, H. Rafaralahy, and M. Darouach, *Convergence Analysis of the Extended Kalman Filter Used as an Observer for Nonlinear Deterministic Discrete-Time Systems*, IEEE Trans. on Autom. Control, 42 (4) (1997) 581-586.

[18]Joonyoung Kim and Kunsoo Huh, *Development of Tire Force Monitoring Systems Using Nonlinear Observers*, Ph.D. Thesis, Hanyang University (1999).